



Published in final edited form as:

Spine (Phila Pa 1976). 2010 April 15; 35(8): 867–873. doi:10.1097/BRS.0b013e3181d74414.

ENGINEERED DISC-LIKE ANGLE-PLY STRUCTURES FOR INTERVERTEBRAL DISC REPLACEMENT

Nandan L. Nerurkar, M.S.¹, Sounok Sen, B.S.^{1,2}, Alice H. Huang, B.S.^{1,2}, Dawn M. Elliott, Ph.D.^{1,2}, and Robert L. Mauck, Ph.D.^{1,2}

¹McKay Orthopaedic Research Laboratory, Department of Orthopaedic Surgery, University of Pennsylvania, Philadelphia, PA 19104

²Department of Bioengineering, University of Pennsylvania, Philadelphia, PA 19104

Abstract

Study Design—Develop construction algorithm in which electrospun nanofibrous scaffolds are coupled with a biocompatible hydrogel to engineer a mesenchymal stem cell (MSC)-based disc replacement.

Objective—Engineer a disc-like angle-ply structure (DAPS) that replicates the multi-scale architecture of the intervertebral disc.

Summary of Background Data—Successful engineering of a replacement for the intervertebral disc requires replication of its mechanical function and anatomic form. Despite many attempts to engineer a replacement for ailing and degenerated discs, no prior study has replicated the multi-scale hierarchical architecture of the native disc, and very few have assessed the mechanical function of formed neo-tissues.

Methods—A new algorithm for the construction of a disc analogue was developed, using agarose to form a central nucleus pulposus and electrospun nanofibrous scaffolds to form the annulus fibrosus region (AF, based on oriented nanofibrous scaffolds). Bovine MSCs were seeded into both regions and biochemical, histological, and mechanical maturation were observed with *in vitro* culture.

Results—We show that mechanical testing in compression and torsion, two loading modalities commonly used to assess disc mechanics, reveal equilibrium and time-dependent behaviors that are qualitatively similar to native tissue, although lesser in magnitude. Further, we demonstrate that cells seeded into the two regions adopt distinct morphologies that mirror those seen in native tissue, and that, in the AF region, this ordered community of cells deposited matrix that is organized in an angle-ply configuration. Finally, constructs demonstrated functional development with long-term *in vitro* culture.

Conclusion—These findings provide a new approach for disc tissue engineering that replicates multi-scale form and function of the intervertebral disc, providing a foundation from which to build a multi-scale, biologic, anatomically and hierarchically relevant composite disc analogue for eventual disc replacement.

Keywords

Tissue engineering; disc replacement; electrospinning; mesenchymal stem cells; mechanics

[†]Corresponding Author: Robert L. Mauck, Ph.D., Assistant Professor of Orthopaedic Surgery and Bioengineering, McKay Orthopaedic Research Laboratory, Department of Orthopaedic Surgery, University of Pennsylvania, 36th Street and Hamilton Walk, Philadelphia, PA 19104, Phone: (215) 898-3294, Fax: (215) 573-2133, lemauck@mail.med.upenn.edu.

Introduction

The intervertebral disc is composed of a central, gelatinous nucleus pulposus (NP) surrounded circumferentially by the annulus fibrosus (AF). Function of the AF is predicated on a high degree of structural organization over multiple length scales: aligned collagen fibers reside within each lamella, and the direction of alignment alternates between adjacent lamellae from $+30^\circ$ to -30° with respect to the transverse axis of the spine, forming an angle-ply laminate structure. This unique microstructure confers to the AF anisotropic mechanical properties and a nonlinear stress-strain profile [1]. The NP is isotropic and composed largely of water and proteoglycans. As a result, the NP exhibits remarkable swelling pressures, but deforms readily in the absence of external constraints such as those present *in vivo*. [2].

Damage and/or degeneration of the disc is a common occurrence, afflicting upward of 97% of the population by 50 years of age [3]. During degeneration, the AF becomes progressively disorganized, concomitant with mechanical and structural failure including tears, fissures, and delamination [4–8], each of which is thought to contribute to low back pain [9, 10]. Treatments for discogenic back pain and disc degeneration are largely palliative, and restoration of function remains unaddressed. Therefore, there is great need for regenerative strategies that may alleviate low back pain while restoring function and range of motion.

A number of disc tissue engineering strategies have emerged over the last decade. Early work focused on the encapsulation of AF and NP cells into hydrogels [11–13]. However, due to the pronounced heterogeneity of disc composition, structure, and function, it is unlikely that a single material can successfully be used to engineer functional replacements for both the AF and NP. Therefore, recent studies have considered distinct strategies for engineering either the NP or the AF [14–21]. Few studies, however, have coupled these two distinct entities to form AF-NP composites [22–24].

Electrospinning permits the fabrication of highly aligned arrays of polymeric nanofibers, whose scale and architecture mimic the natural organization of many fiber-reinforced soft tissues such as muscle, tendon, the knee meniscus, and the AF [11]. These scaffolds can be manufactured to possess key mechanical behaviors of fiber-reinforced soft tissues including nonlinearity, anisotropy, and finite elastic deformations [12]. Moreover, fiber alignment in the scaffold guides alignment of resident cells and ordered deposition of extracellular matrix (ECM) [34–36]. Attachment and proliferation on electrospun scaffolds have been observed for bovine and human AF cells and mesenchymal stem cells (MSCs) [13–15]. Our group has employed aligned nanofibrous scaffolds to engineer single lamellar AF constructs [16], and more recently, to fabricate bi-lamellar tissues that replicate the angle-ply fiber organization of the native tissue [17]. However, little has been done with electrospinning for AF-NP composite tissue engineering [24]. Of the few studies to engineer whole disc composites, thus far none have successfully replicated the unique multi-scale architecture of the native tissue. As a result, native disc mechanical properties have not been achieved. Because the disc functions primarily as a load-bearing tissue, it is imperative that engineered constructs successfully match the native mechanical properties if tissue engineering is to ascend to the stage of clinical implementation.

In the present study, we employed electrospun scaffolds to develop a multi-lamellar engineered tissue that replicates the multi-scale architecture of the native AF. We coupled this AF-like structure with a biocompatible hydrogel for the NP, and so created a composite disc-like angle-ply structure (DAPS). Formation and study of these DAPS was carried out in three steps: 1) an *acellular* study to establish the method by which DAPS could be

constructed and mechanically tested via torsion and unconfined compression; 2) a *short-term* culture study in which DAPS were seeded with bovine AF cells; and 3) a *long-term in vitro* study with MSCs seeded within each region, to determine the functional maturation of the DAPS via histological, biochemical, and mechanical evaluation. Results from this study provide a foundation from which to build a multi-scale, biologic, anatomically and hierarchically relevant composite DAPS for eventual disc replacement.

Materials and Methods

(1) Acellular Study: DAPS Fabrication and Mechanical Testing

To generate the AF region of the acellular DAPS, poly(ϵ -caprolactone) (PCL, Sigma Aldrich, batch # 00702CE) fiber mats (~250 μ m thick) were electrospun as previously described [39, 41]. Briefly, the PCL solution was extruded at 2.5 mL/h through a spinneret charged to +13 kV, generating a nanofibrous jet that was collected onto a grounded mandrel rotating at 10 m/s to instill alignment in the depositing fibers [18]. Rectangular samples (3 mm \times 30 mm) were excised from the mesh along the fiber direction.

Strips were spot-welded end-to-end with parallel fiber alignment using a soldering iron to achieve 150 mm long strips [19]. Strips were wrapped concentrically within a custom mold by feeding one end into a slotted core (5 mm diameter), which was then rotated (Fig. 1A) until an outer diameter of 10 mm was achieved. Rabbit disc and NP area were used to define these geometries [20]. The core was then removed and the space filled with 5% agarose. To determine the contribution of the NP in the acellular DAPS, a 5% agarose gel was also cast in the shape of the NP region of the DAPS.

Acellular DAPS and agarose-only NP (5 mm diameter \times 3 mm height) samples were tested in compression and torsion. Compression was applied by applying 25% total axial strain in 5% increments at 1%/sec, with 10 min relaxation between steps. Torsional testing was performed on a custom-built micro-torsion device [21]. Each construct was compressed to 25% axial strain and allowed to relax for 5 min. 10 cycles of $\pm 6^\circ$ torsion were applied at 0.05 Hz [21]. Torque and rotation data are presented from the 10th cycle. All testing was performed in a phosphate buffered saline (PBS) bath.

(2) Short-term Culture Study: AF Cell Isolation and Analysis of Cell-Seeded DAPS

Bovine outer AF cells were isolated and expanded as described previously [16]. A similar construction method to that described above was followed, now using oriented fiber strips that were excised 30° from the fiber direction. Doing so produces scaffolds with an organization of fibers similar to the organization of the native AF [17]. Strips were seeded at 1.5×10^6 cells per side and pre-cultured in a serum-free, chemically defined growth media supplemented with 10 ng/mL TGF- $\beta 3$ for one week [22]. The AF region of the DAPS was formed by coupling two strips with opposing orientations of $\pm 30^\circ$ and wrapping as above, such that each rotation increased the lamellar number by 2, with alternating fiber directions (Fig. 1A).

These AF-only constructs were cultured for 7 days after wrapping in chemically defined medium (above), then dehydrated and imaged by SEM (n=2) or embedded in Optimal Cutting Temperature (OCT) freezing medium and cryotomed to 8 or 25 μ m thickness (n=2). A subset of samples was sectioned obliquely to visualize in-plane cell and collagen orientations across lamellar interfaces. Sections were stained for cell nuclei (DAPI) and/or filamentous actin (AlexaFluor-phalloidin) or for collagen (Picosirius Red). DAPI and actin-stained sections were visualized at 20X on a Nikon T30 inverted fluorescent microscope. Picosirius Red stained sections were viewed on an upright Leica DMLP microscope.

(3) Long-term Study: Functional Maturation of MSC-Seeded DAPS

Bone marrow was isolated from femurs and tibiae of 3–6 month old calves [23], then plated on tissue culture plastic in basal medium. After initial colony formation, MSCs were expanded to passage 2 (above). Strips (30° orientation) were seeded with bovine MSCs at –2 weeks as above. At 0 weeks, strips were paired into bi-layers with opposing +/-30° fiber orientations and wrapped concentrically (above, Fig. 1A). After 1 week, the central lumen (5 mm diameter) was filled with MSCs encapsulated in 2% agarose at a 20×10^6 cells/mL [24]. Fully formed DAPS were cultured for an additional 6 weeks in chemically defined media with 10 ng/mL TGF- β 3. At 1 week, NP-only discs seeded with MSCs were also formed (5 mm diameter and 3 mm thickness), and cultured identically and in parallel to determine the effect of the AF region on NP growth and maturation in the DAPS.

At 1, 3, and 6 weeks after formation, two samples were frozen in OCT, cryotomed axially to 16 μ m thickness, and stained with DAPI, Alcian Blue, and Picrosirius Red. Additional samples were sectioned obliquely, stained with Picrosirius Red, and visualized via polarized light microscopy [25].

DAPS were tested in unconfined compression using a custom device (n=4) [2]. Samples were pre-equilibrated for 5 minutes with a creep load of 2 grams, followed by the application of a single 10% axial compressive strain at 0.05%/sec, followed by 1000 seconds of relaxation. Equilibrium modulus was derived from the equilibrium stress and the sample geometry, and the percent relaxation from peak to equilibrium stress. After mechanical testing, DAPS were separated into AF and NP sub-regions, which were assayed for collagen, GAG, and DNA content [22]. Lapine lumbar AF and NP (n=5) plugs were included to provide native tissue concentrations of these biochemical constituents.

Statistical Analysis

Significant differences between DAPS and agarose-only samples were determined by t-test in the acellular study (1). In the long-term study (3), a two-way ANOVA with Tukey's post hoc test ($p < 0.05$) was used to determine significance, with independent variables of culture duration and sample type (agarose-only vs. DAPS). All results are reported as mean \pm standard deviation.

Results

DAPS replicated the gross anatomic form of the disc, including an angle-ply AF and a gelatinous NP (Fig. 1B, C). DAPS exhibited compressive stress relaxation and nonlinear torsion responses (Fig. 1D, E), two traits of native disc [21, 26, 27]. Compressive and shear moduli were an order of magnitude higher for the DAPS than for the NP-only agarose. In short-term *in vitro* culture with bovine AF cells, AF regions successfully replicated the meso-scale multi-lamellar structure of the native tissue (Fig. 2A). Matrix deposition was evident at the lamellar interfaces (Fig. 2B). At this early time point of culture, cells colonized the interface, with limited infiltration to intra-lamellar compartments. Oblique histological sections through the interface showed actin organized in opposing directions in adjacent lamellae (Fig. 2C). Picrosirius Red staining likewise showed oriented collagen deposition along these alternating directions (Fig. 2D).

Next, long-term culture studies were performed with DAPS containing both an MSC-seeded AF and a gelatinous MSC-seeded NP. DAPI staining after 1 week revealed MSCs distributed throughout the NP and at lamellar boundaries in the AF (Fig. 3A). By 6 weeks, DAPS had matured with prominent deposition of ECM in both the NP and AF regions. Polarized light microscopy of Picrosirius Red-stained oblique sections showed successful replication of native angle-ply collagen architecture, indicated by the alternating birefringent

hues in adjacent lamellae (Fig. 3B). GAG (Fig. 4A, C) and collagen (Fig. 4B, D) accumulated in both regions. Notably, staining for both molecules appeared to decrease in intensity with progression from the outer AF inward.

At 1 week, DNA content was higher in the AF region, which had been pre-cultured for 2 weeks prior to the addition of the NP region (Fig. 5A, $p < 0.05$). DNA content increased in the NP region with culture, but did not change further in the AF. Similarly, GAG and collagen content increased in the NP region with culture duration (Fig. 5B, C), and were higher in the AF region at 1 week, due again to ongoing matrix deposition in this region during the pre-culture period. At 6 weeks, GAG content in the NP and AF regions were not different, but both were higher than at 1 week ($p < 0.05$). Conversely, collagen content remained higher in the AF region throughout the culture period. By 6 weeks, the DAPS attained DNA contents in both the NP and AF region that were similar to native disc. However, GAG content reached only ~25% of native tissue levels for both NP and AF (~1.2% wet weight, WW for both regions of the DAPS, ~3.8% WW for native AF, ~4.6% WW for native NP). Collagen content, which is 200 times higher in native AF than NP, showed a mixed result; NP collagen content in the DAPS was higher than that measured for native NP (~0.4 vs. ~0.1% WW), while AF collagen in the DAPS was lower than that measured for native AF (~1% vs. 20% WW).

ECM in the NP-region of the DAPS was lower when compared to MSC-seeded NP-only constructs cultured in the absence of a confining AF region ($0.97 \pm 0.09\%$ WW collagen and $2.32 \pm 1.1\%$ WW GAG at 6 weeks). Interestingly, DNA content was not significantly different between the NP of DAPS and the NP-only constructs.

DAPS equilibrium modulus increased over two-fold to 45 kPa by 6 weeks (Fig. 6A, $p < 0.05$). Likewise, % relaxation increased over this same time course (Fig. 6B, $p < 0.05$, from ~40% to ~60%). NP-only constructs cultured without an AF region reached 148 kPa and 72 % relaxation.

Discussion

In this study, MSC-seeded nanofibrous scaffolds were coupled with an engineered MSC-seeded NP to create a DAPS that replicated the multi-scale anatomic form of the native disc, including an angle-ply AF region. These constructs mirrored several important functional signatures of the native disc, and with long-term *in vitro* culture, accrued collagen and GAG within both AF and NP regions, resulting in a two-fold increase in compressive modulus.

Investigation of the mechanics of acellular DAPS demonstrated an improvement in mechanical function when the electrospun AF region was used to reinforce the central agarose NP, indicating that these two regions interact to elicit mechanical responses in compression and torsion that mirror native disc, even prior to ECM deposition. Such structural measures are critical metrics for determining functional equivalence to healthy disc. While strategies that aim to engineer the AF or NP alone may replicate regional properties of the native tissue, these two disparate tissues must ultimately be integrated and evaluated in the context of a higher order of functionality.

In short-term culture of AF regions, cells adopted an elongated morphology and were oriented in parallel within each lamella, with the direction of alignment alternating between adjacent lamellae. Cell shape and organization closely mimic that of AF precursor cells during development of the embryonic disc [28]. ECM deposition was organized along the local direction of cell alignment, resulting in collagen rich lamellae that replicated the angle-ply organization of the native AF. With long-term culture, substantial accumulation of

collagen and GAG – the two primary components of native disc – was observed. This matrix accumulation resulted in a doubling of the compressive modulus within 6 weeks of culture.

While relatively few groups have sought to engineer an entire disc [22–24], even fewer have considered mechanical properties in any context. In one exception, a composite disc was engineered by encapsulating NP cells in alginate surrounded by an AF cell-seeded scaffold of polylactic acid reinforced polyglycolic acid [29, 30]. Although biochemical content approached native levels and compressive mechanical properties increased with subcutaneous implantation, disc-level mechanics were not measured, and the angle-ply architecture of the native AF was not achieved. The work presented in the current study represents the first whole-disc replacement to replicate this microarchitecture of the disc, and the only study since the foundational work of Mizuno et al. to show enhanced mechanical behavior in an AF-NP composite [30].

Although the present work demonstrates unique advances in disc tissue engineering, it also highlights several challenges that must be addressed if regenerative medicine is to influence clinical treatment of disc degeneration and low back pain. While biochemical content increased in DAPS, it did not reach native levels (particularly for collagen in the AF) and deposition appeared dependent on radial position. Moreover, ECM accumulation was severely retarded within the NP of DAPS compared to agarose-only, MSC-seeded cylinders of the same size as the NP region, indicating a prohibitive effect of the surrounding AF region on growth in the NP region. This is likely indicative of nutrient limitations in these larger constructs. Such diffusional challenges have long hindered progress in disc organ culture studies, where the native disc is so large and dense that, under *in vitro* culture conditions, tissue health and matrix biosynthesis cannot be easily sustained [31]. Nutrient and waste exchange is a critical issue that must be considered for any engineered disc replacement that aims to recreate the composition and scale of the native tissue. Moreover, given the nutrient limitations implicit in the native tissue environment, this finding may be exacerbated with *in vivo* implantation, where diffusion through the axial implant surfaces would be further reduced by the presence of vertebral bodies. Dynamic culture in mechanical loading bioreactors or convection-facilitated transport may be required to overcome this limitation *in vitro* [32]. For future implantation into the disc space *in vivo*, it may be necessary to develop techniques that provide for efficient nutrient exchange between the engineered disc and the vascular source that underlies the endplate.

Alternative materials might also be used to enhance DAPS maturation. For instance, in the current construction, while collagen was deposited at the interface of between each pair of lamellae, cellular infiltration and matrix formation were limited to these boundaries. Cellular ingress might be improved with the incorporation of sacrificial nanofibers into the scaffold [42, 53]. Additionally, while agarose was employed in this study, there exist a range of alternatives that could be used in its place [33].

In order to compare DAPS mechanics with the native disc, it will be necessary to test the isolated disc. However, excision of the disc from its neighboring vertebrae alters its function: the NP depressurizes and collagen fibers of the AF are no longer anchored at their ends. This not only hampers the determination of native tissue benchmarks, but emphasizes the complexity of disc tissue engineering. To properly assess the function of AF and NP constructs, they must not only be coupled, but for the most informed approach, must be fabricated with anatomic boundary constraints. As the current technology moves toward *in vivo* application, it will be critically important to develop suitable boundaries for integration with the surrounding vertebrae, as well as the physiologic constraints necessary to appropriately assess functional performance. While these obstacles are considerable, the

present work provides a point of initiation, a test-bed in which to begin addressing these challenges for engineered disc replacement.

Acknowledgments

The authors gratefully acknowledge An M. Nguyen and Amy S. Orlansky for their assistance with data collection. This work was funded by the National Institutes of Health (EB02425), Penn Center for Musculoskeletal Disorders (AR050950), and the National Science Foundation (AHH).

References

1. Elliott DM, Setton LA. Anisotropic and inhomogeneous tensile behavior of the human annulus fibrosus: experimental measurement and material model predictions. *J Biomech Eng.* 2001; 123:256–263. [PubMed: 11476369]
2. Johannessen W, Elliott DM. Effects of degeneration on the biphasic material properties of human nucleus pulposus in confined compression. *Spine (Phila Pa 1976).* 2005; 30(24):E724–729. [PubMed: 16371889]
3. Miller JA, Schmatz C, Schultz AB. Lumbar disc degeneration: correlation with age, sex, and spine level in 600 autopsy specimens. *Spine.* 1988; 13(2):173–178. [PubMed: 3406837]
4. Acaroglu ER, Iatridis JC, Setton LA, Foster RJ, Mow VC, Weidenbaum M. Degeneration and aging affect the tensile behavior of human lumbar annulus fibrosus. *Spine.* 1995; 20(24):2690–2701. [PubMed: 8747247]
5. Ebara S, Iatridis JC, Setton LA, Foster RJ, Mow VC, Weidenbaum M. Tensile properties of nondegenerate human lumbar annulus fibrosus. *Spine.* 1996; 21(4):452–461. [PubMed: 8658249]
6. Fujita Y, Duncan NA, Lotz J. Radial tensile properties of the lumbar annulus fibrosus are site and degeneration dependent. *Journal of Orthopaedic Research.* 1997; 15:814–819. [PubMed: 9497805]
7. Elliott DM, Setton LA. Anisotropic and inhomogeneous tensile behavior of the human annulus fibrosus: experimental measurement and material model predictions. *J Biomech Eng.* 2001; 123(3): 256–263. [PubMed: 11476369]
8. Guerin HL, Elliott DM. Quantifying the contributions of structure to annulus fibrosus mechanical function using a nonlinear, anisotropic, hyperelastic model. *J Orthop Res.* 2007; 25(4):508–516. [PubMed: 17149747]
9. Marchand F, Ahmed AM. Investigation of the laminate structure of lumbar disc annulus fibrosus. *Spine.* 1990; 15(5):402–410. [PubMed: 2363068]
10. Bogduk N. The lumbar disc and low back pain. *Neurosurg Clin N Am.* 1991; 2(4):791–806. [PubMed: 1821758]
11. Mauck RL, Baker BM, Nerurkar NL, Burdick JA, Li WJ, Tuan RS, Elliott DM. Engineering on the Straight and Narrow: The Mechanics of Nanofibrous Assemblies for Fiber-Reinforced Tissue Regeneration. *Tissue Eng Part B Rev.* 2009
12. Nerurkar NL, Elliott DM, Mauck RL. Mechanics of oriented electrospun nanofibrous scaffolds for annulus fibrosus tissue engineering. *J Orthop Res.* 2007; 25(8):1018–1028. [PubMed: 17457824]
13. Yang L, Kandel RA, Chang G, Santerre JP. Polar surface chemistry of nanofibrous polyurethane scaffold affects annulus fibrosus cell attachment and early matrix accumulation. *J Biomed Mater Res A.* 2008
14. Gruber HE, Hoelscher G, Ingram JA, Hanley EN Jr. Culture of human annulus fibrosus cells on polyamide nanofibers: extracellular matrix production. *Spine.* 2009; 34(1):4–9. [PubMed: 19127155]
15. Nesti LJ, Li WJ, Shanti RM, Jiang YJ, Jackson W, Freedman BA, Kuklo TR, Giuliani JR, Tuan RS. Intervertebral disc tissue engineering using a novel hyaluronic acid-nanofibrous scaffold (HANFS) amalgam. *Tissue Eng Part A.* 2008; 14(9):1527–1537. [PubMed: 18707229]
16. Nerurkar NL, Mauck RL, Elliott DM. ISSLS prize winner: Integrating theoretical and experimental methods for functional tissue engineering of the annulus fibrosus. *Spine (Phila Pa 1976).* 2008; 33(25):2691–2701. [PubMed: 19018251]

17. Nerurkar NL, Baker BM, Sen S, Wible EE, Elliott DM, Mauck RL. Nanifibrous Biologic Laminates Replicate the Form and Function of the Annulus Fibrosus. *Nature Materials*. 2009;10:1038/NMAT2558
18. Baker BM, Gee AO, Metter RB, Nathan AS, Marklein RA, Burdick JA, Mauck RL. The potential to improve cell infiltration in composite fiber-aligned electrospun scaffolds by the selective removal of sacrificial fibers. *Biomaterials*. 2008; 29(15):2348–2358. [PubMed: 18313138]
19. Baker, BM.; O'Connell, GD.; Sen, S.; Nathan, A.; Elliott, DM.; Mauck, RL. Multi-Lamellar and Multi-Axial Maturation of Cell-Seeded Fiber-Reinforced Tissue Engineered Constructs. *Proceedings of ASME 2007 Summer Bioengineering Conference*; Keystone, CO. June 20–24; 2007.
20. O'Connell GD, Vresilovic EJ, Elliott DM. Comparison of animals used in disc research to human lumbar disc geometry. *Spine*. 2007; 32(3):328–333. [PubMed: 17268264]
21. Espinoza Orias AA, Malhotra NR, Elliott DM. Rat disc torsional mechanics: effect of lumbar and caudal levels and axial compression load. *Spine J*. 2009; 9(3):204–209. [PubMed: 18495544]
22. Mauck RL, Yuan X, Tuan RS. Chondrogenic differentiation and functional maturation of bovine mesenchymal stem cells in long-term agarose culture. *Osteoarthritis Cartilage*. 2006; 14(2):179–189. [PubMed: 16257243]
23. Baker BM, Mauck RL. The effect of nanofiber alignment on the maturation of engineered meniscus constructs. *Biomaterials*. 2007; 28(11):1967–1977. [PubMed: 17250888]
24. Huang AH, Yeger-McKeever M, Stein A, Mauck RL. Tensile properties of engineered cartilage formed from chondrocyte- and MSC-laden hydrogels. *Osteoarthritis Cartilage*. 2008; 16(9):1074–1082. [PubMed: 18353693]
25. Thomopoulos S, Williams GR, Gimbel JA, Favata M, Soslowky LJ. Variation of biomechanical, structural, and compositional properties along the tendon to bone insertion site. *J Orthop Res*. 2003; 21:413–419. [PubMed: 12706013]
26. Beckstein JC, Sen S, Schaer TP, Vresilovic EJ, Elliott DM. Comparison of animal discs used in disc research to human lumbar disc: axial compression mechanics and glycosaminoglycan content. *Spine (Phila Pa 1976)*. 2008; 33(6):E166–173. [PubMed: 18344845]
27. Johannessen W, Cloyd JM, O'Connell GD, Vresilovic EJ, Elliott DM. Trans-endplate nucleotomy increases deformation and creep response in axial loading. *Ann Biomed Eng*. 2006; 34(4):687–696. [PubMed: 16482409]
28. Hayes AJ, Benjamin M, Ralphs JR. Role of actin stress fibres in the development of the intervertebral disc: cytoskeletal control of extracellular matrix assembly. *Dev Dyn*. 1999; 215(3): 179–189. [PubMed: 10398529]
29. Mizuno H, Roy AK, Vacanti CA, Kojima K, Ueda M, Bonassar LJ. Tissue-engineered composites of anulus fibrosus and nucleus pulposus for intervertebral disc replacement. *Spine*. 2004; 29(12): 1290–1297. discussion 1297-1298. [PubMed: 15187626]
30. Mizuno H, Roy AK, Zaporozhan V, Vacanti CA, Ueda M, Bonassar LJ. Biomechanical and biochemical characterization of composite tissue-engineered intervertebral discs. *Biomaterials*. 2006; 27(3):362–370. [PubMed: 16165204]
31. Risbud MV, Izzo MW, Adams CS, Arnold WW, Hillibrand AS, Vresilovic EJ, Vaccaro AR, Albert TJ, Shapiro IM. An organ culture system for the study of the nucleus pulposus: description of the system and evaluation of the cells. *Spine*. 2003; 28(24):2652–2658. discussion 2658-2659. [PubMed: 14673364]
32. Nerurkar, NL.; Sen, S.; Baker, BM.; Zachry, TL.; Elliott, DM.; Mauck, RL. Dynamic culture enhances stem cell ingress and extracellular matrix deposition on electrospun nanofibrous scaffolds. *Transactions of the 56th Annual Meeting of the Orthopaedic Research Society*; New Orleans, LA. 2010.
33. Erickson IE, Huang AH, Chung C, Li RT, Burdick JA, Mauck RL. Differential Maturation and Structure-Function Relationships in MSC- and Chondrocyte-Seeded Hydrogels. *Tissue Eng Part A*. 2009

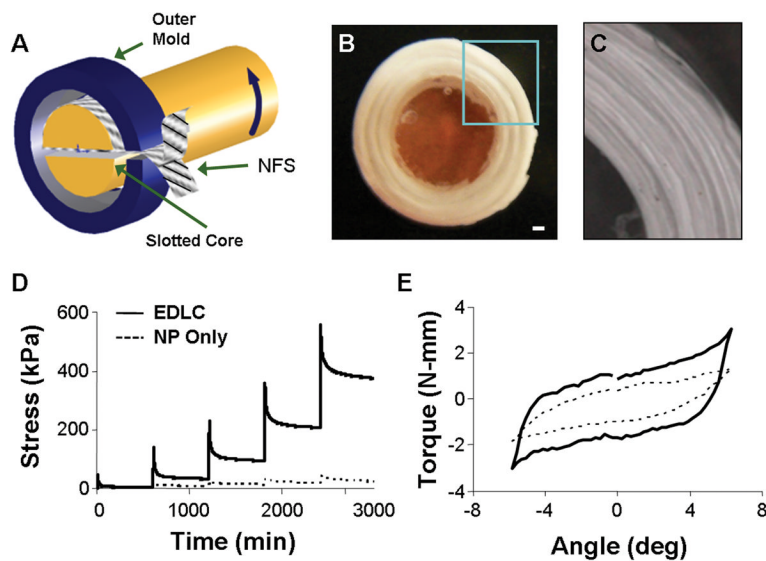


Figure 1. (A) Schematic showing of fabrication process for formation of engineered disc-like angle-ply structure (DAPS) (NFS: nanofibrous scaffold). (B) Gross morphology of DAPS with nanofibrous AF region and agarose NP region, scale bar: 1 mm. (C) Close up view of AF region enlarged from box in (B). Representative stress-relaxation (D) and torsion (E) response of DAPS showing the viscoelastic and non-linear response of the composite.

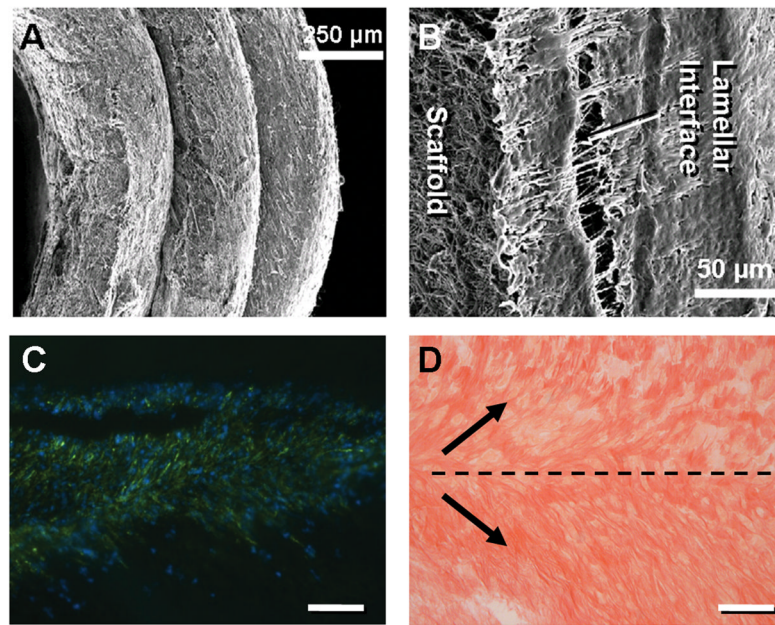


Figure 2. (A) SEM of AF region after 1 week of culture. (B) Higher magnification SEM of interface formation between individual lamellae at 1 week time point. Actin (green) and DAPI (blue) staining of cells (C) and Picrosirius Red staining of newly formed collagen (D) organized in alternating directions along interface within sections taken oblique to the axial plane. Scale bar: 250 microns.

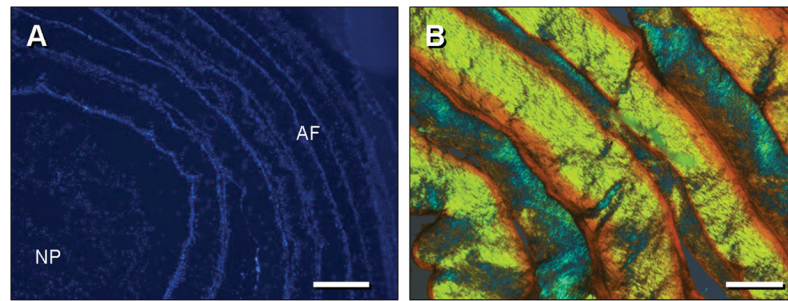


Figure 3. (A) DAPI staining of transverse section of DAPS at 1 week, showing homogenous distribution of MSCs in the 'NP' region, and lamellar organization of MSCs in the 'AF' region. Scale: 500 microns. Note: separation of NP and AF occurred as an artifact of sectioning. (B) Polarized light image of Picrosirius Red-stained oblique section of 'AF' region at 6 weeks showing birefringent material in opposing orientations with progression through adjacent lamellae. Scale: 100 (C) and 250 (D) microns.

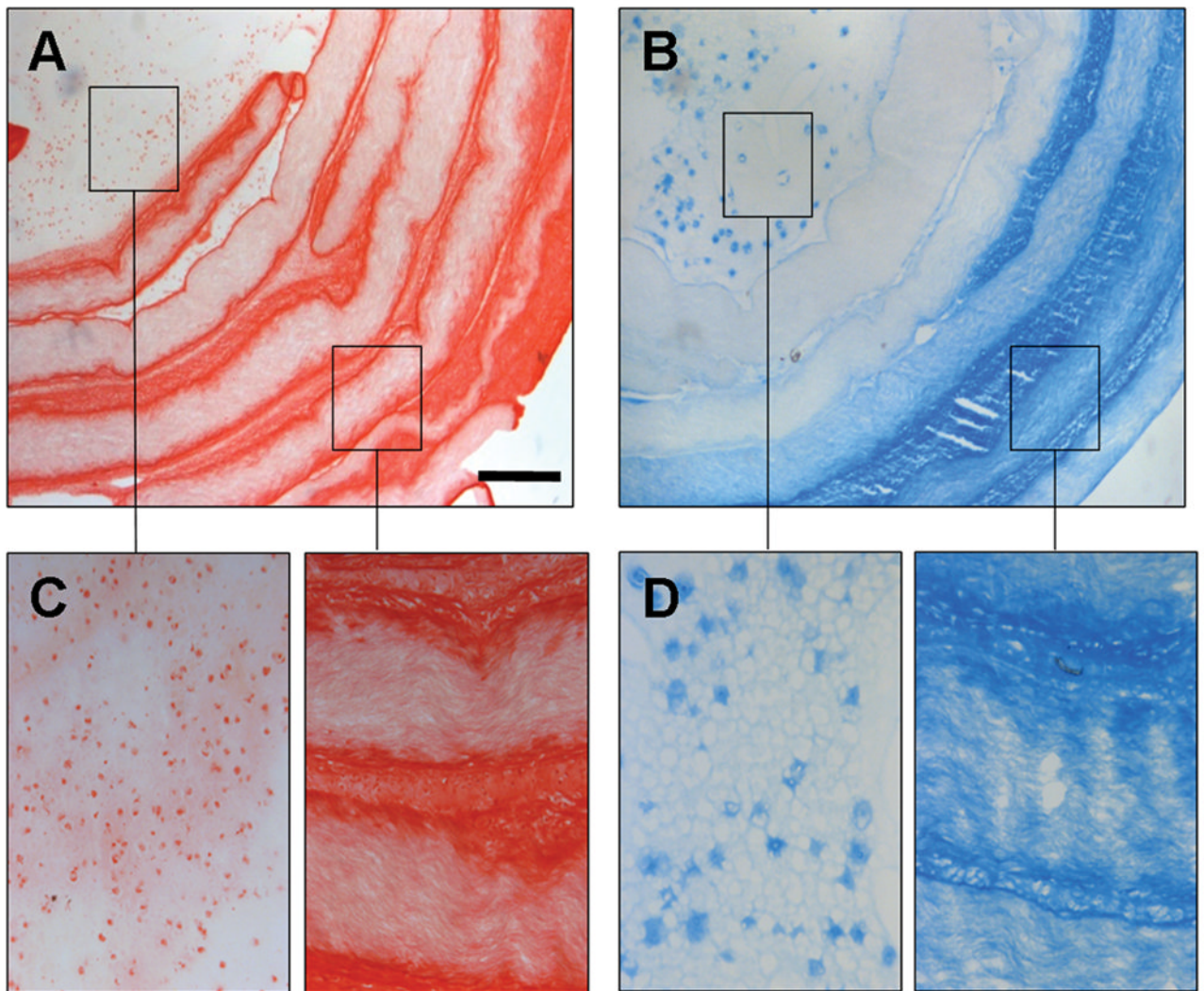


Figure 4. Alcian Blue (A) and Picrosirius Red (B) staining of 6 week constructs with magnified images from NP and AF regions shown in (C) and (D) as indicated. Scale = 500 microns (A–B), 125 microns (C–D).

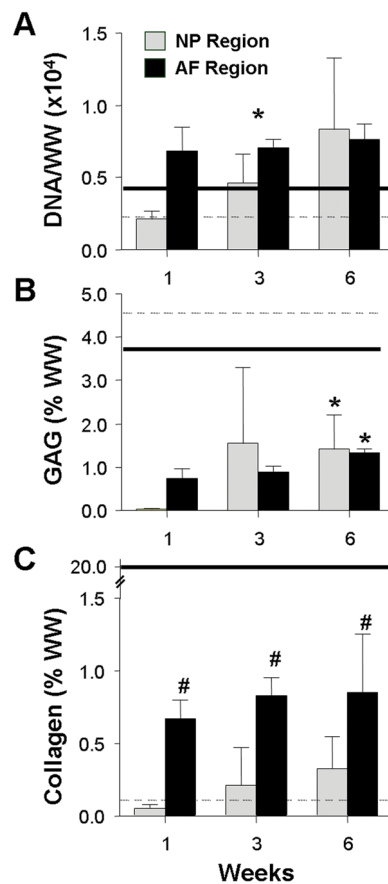


Figure 5. DNA (A), GAG (B), and collagen (C) content, reported in % wet weight (% WW) for the 'NP' and 'AF' regions as a function of time in culture. Solid and dashed lines indicate native lapine AF and NP benchmarks, respectively. # indicates $p < 0.05$ for compared to time-matched 'NP' values; * indicates $p < 0.05$ for compared to 1 week time point. Results presented as the mean \pm SD for 4 samples/group per time point.

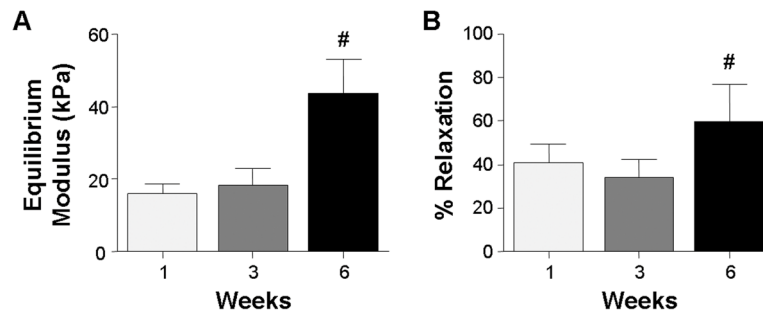


Figure 6. Equilibrium modulus (A) and percent stress relaxation (B) measured by unconfined compression for the DAPS as a function of time. # indicates $p < 0.05$ compared to the 1 week time point. Results presented as the mean \pm SD for 4 samples/group per time point.